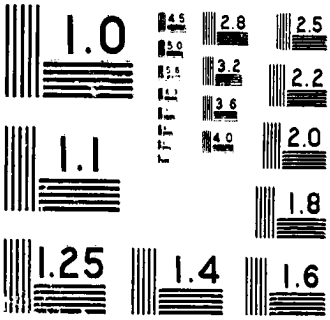

NASA TECHNICAL MEMORANDUM

NASA TM X-71574

NASA TM X-71574

SOME COMPARISONS OF THE FLOW CHARACTERISTICS OF A TURBOFAN COMPRESSOR SYSTEM WITH AND WITHOUT INLET PRESSURE DISTORTION

by David G. Evans, Claude E. deBogdan,
Ronald H. Soeder and E. J. Pleban
Lewis Research Center
Cleveland, Ohio 44135

TECHNICAL PAPER proposed for presentation at
SQUID/Air Force Office of Scientific Research/United Aircraft
Research Laboratory Workshop on Unsteady Flows in Jet Engines
East Hartford, Connecticut, July 11-12, 1974

SOME COMPARISONS OF THE FLOW CHARACTERISTICS OF A TURBOFAN COMPRESSOR SYSTEM WITH AND WITHOUT INLET PRESSURE DISTORTION

by David G. Evans, Claude E. deBogdan, Ronald H. Soeder and E. J. Pleban

NASA-Lewis Research Center
Cleveland, Ohio

E-8018

ABSTRACT

The measured effects of a circumferential distortion in inlet total pressure on the fan, low, and high compressor of an afterburning turbofan engine are presented and discussed. Extensive inner-stage instrumentation, combined with a unique test technique offered an accurate means of measuring the shifts in flow, performance, and stall mechanisms within the compressor. These effects are compared at one speed to the corresponding effects measured with undistorted inlet flow. The results show the rate at which the distorted flow areas were attenuated and rotated, as well as the change in flow velocities that occurred at various points in the compressor. High response pressure traces indicated the location of stalls including the sequence of dynamic events from the onset and propagation of various stall-recovery events, to compressor surge, to the resulting hammershock.

INTRODUCTION

The effects of inlet flow distortion on the performance and stability of aircraft gas turbine compressor systems has long been an important consideration in engine development programs. In support of this, an extensive program has been in progress at the Lewis Research Center to evaluate the effects of inlet distortion on various types of engines, including the turbojet and the more complex types of turbofan engines. This paper is directed towards one aspect of the program where a 180 degree circumferential square wave in inlet total pressure distortion was imposed upstream of a TF30-P3 afterburning turbofan engine, shown in figure 1. The effects of the inlet distortion on the flow characteristics within the compressor system were measured and compared to its operation with an undistorted inlet.

The results of the tests are currently being analyzed. However, the data indicate the shifts in the flow conditions and stall mechanisms that occur within the compressor system due to the distorted inlet. Implied in the results are the influence that the design and performance characteristics of the compressor system have on the way in which the flow reacts to the distortion. That is, the way in which the compressor stage characteristics, stage exit volumes, cavities adjacent to the flow path, and the propagation of the flow defect areas effect the compressor inner-stage distortion attenuation, combined distortion profiles, flow velocities, overall compressor performance, and the location and type of dynamic events that occur during surge. These data and results are discussed in the following sections.

INSTRUMENTATION AND PROCEDURE

During the test, the engine was first operated with an undistorted inlet, and the flow properties measured at each of the rating stations shown in figure 1. The measured properties were total and static pressure and total temperature. The instrumentation at station 2 consisted of 8 rakes having elements at 5 radial positions, 8 tip wall static taps, and 4 hub wall static taps. Inner-stage rakes having both steady-state and high response elements at various radial positions, and tip wall static taps, were located in stator channels on the left and right sides of the compressor system approximately 180 degrees opposed. Engine mass flow and bypass ratio was determined from

measurements taken ahead of station 2, and at station 3.

The engine was then driven into stall by applying back pressure to the core compressor by either inflowing high pressure air to the primary combustor diffuser, or by fuel-pulsing the primary combustor. During the stall, high response pressure measurements were recorded throughout the compressor system to determine the location and sequence of the dynamic events.

The engine was next operated with the 180 degree extent circumferential distortion in inlet total pressure, created by continuously controlling the airflow to 3 of the 60 degree segments of the air-jet system shown in figure 1. The distortion was rotated step-wise around the inlet in 60 degree steps. The amplitude, extent, and shape of the distorted sector was held constant while the data was recorded between each step. This procedure provided the close circumferential spacing between data points needed to define the circumferential variation in the flow conditions at each station. The amplitude of the inlet distortion was held constant at a value of (DELTA PT/PT AVE) of approximately 9 percent, which was approximately 2/3 of the amplitude required to stall the engine. Then, after making six steps to complete a circumferential traverse of the distorted sector around the inlet, the position and extent of the distorted sector was held constant, and its amplitude increased until the engine stalled. Stall occurred at a distortion amplitude of approximately 13 percent.

During the various phases of the test, the engine operating conditions were held nominally at:

Inlet Reynolds No. Index, RNI...0.5
Low rotor corrected speed.....8640
(90 percent design)
High rotor corrected speed.....10200
Primary jet nozzle area.....3.76 feet square
(100 percent design)
Compressor bleeds.....Closed

RESULTS AND DISCUSSION

Inlet Flow Conditions

Figure 2 shows the circumferential variation in inlet flow properties measured during the step-wise rotation of the distorted inlet sector. The data points shown in figure 2(a) illustrate the degree of circumferential coverage and data resolution achieved with this technique. (Symbols are defined in APPENDIX A.) The air-jet device produced a nearly square variation in inlet total pressure, and a sinusoidal variation in static pressure shown in figure 2(b). The resultant effect on the calculated variation in flow velocity at station 2 is shown in figure 2(c).

The amplitude of the static pressure variation, figure 2(b), increased as the flow progressed towards the engine face due to the strong pumping effect of the engine; that is, the distorted and undistorted sides of the compressor system operated at the same corrected speed, and therefore attempted to operate at close to the same corrected mass flow and Mach No. on both sides. The variation in inlet static pressure implies that a driving force existed in the circumferential direction that could turn the flow towards the center of the distorted sector in both the free-stream and wall boundary layers immediately upstream of the engine. In this test, flow angles were not measured. However, inlet deviation angles in the free-stream of up to 20 degrees from axial have been measured in single stage tests, references 1 to 3.

Compressor Flow Conditions

The data presented in this section for operation with a distorted inlet were obtained by the procedure noted in the INTRODUCTION, and have the inlet characteristics noted in figure 2. Plots of several typical inner-compressor circumferential profiles of pressure and temperature are shown in figure 3. They show the difference in the amplitude and circumferential location of two inner-stage pressures as compared to the location of the inlet distortion. Also shown is an example of the temperature distortion which resulted within the compressor system due to the higher pressure ratio and heat of compression on the pressure distorted side of the engine.

The next four figures, 4 through 7, show the attenuation of the amplitude of the inlet distortion, and the rotation of the distorted sector within the compressor system. They were obtained from plots of all the inner-compressor data, similar to the three measurements shown in figure 3. Figure 4(a) shows the attenuation of the distortion at each station. Starting with the

inlet distortion of approximately 9 percent amplitude at the inlet, the fan and compressors linearly attenuated the amplitude to 2 percent at the high compressor exit, station 4. From stations 2 to 2.3, attenuation was more rapid in the fan stream than the core stream. This may have been due to the larger plenum and hence lower level of static pressure distortion behind the fan stream than in the core stream at station 2.3, figure 4(b), plus the presumption that the higher blade speed of the portion of the blading in the fan stream would exhibit a stronger pumping effect on the flow in the fan stream than in the core stream.

Figure 4(a) also shows some amplification in distortion at the hub between the low and high compressors, station 3. The cause is not apparent. However, it may be due to some performance characteristic of the hub region of the aft stages of the low compressor causing the distortion to be amplified rather than attenuated. It could also be due to the possible occurrence of secondary flows (cross-flows) within the various annular cavities adjacent to the low compressor flow path at the hub, such as may be noted in figure 1 at and between stations 2.3 and 3. The driving force for such flows would be the circumferential variation in static pressure that exists at these stations. The mechanism for causing the increase in total pressure distortion would be the radial impingement of the cross-flows back into the compressor flow path on the low static pressure side of the compressor. This circumferential relationship between the hub amplification and the low static pressure regions is shown in later figures (6 and 7).

The circumferential variation in the tip wall static pressure, figure 4(b), indicates two effects that are occurring. First; the relatively large volumes in the flow path behind the fan, low, and high pressure compressors, stations 2.3, 3, and 4, respectively, act as plenums which reduce the amplitude of the variation in static pressure to less than 2 percent. Second; the front stages of the fan and low compressor located just behind stations 2 and 2.3, respectively, have a strong pumping effect on the flow which increase the amplitude of the static pressure distortion to approximately the level of the total pressure distortion at these stations. This pumping effect increased the attenuation of the circumferential variation in the absolute flow velocity entering these stage groups. The circumferential variation in velocity is noted in figure 4(c), where the inner-stage flow velocities were calculated from the measured free-stream total pressures and temperatures, and tip wall static pressures, assuming non-rotational flow.

Figure 4(d) shows the build-up in the circumferential variation of temperature due to the difference in pressure ratio and heat of compression between the two sides of the distorted compressor system. The build-up was not linear as might be expected, but occurred across the forward part of the compressor system where the circumferential differences in total pressure were the largest.

The radial variation in the circumferential total pressure distortion at several of the stations within the compressor is shown in figure 5. A moderate amount of radial distortion was produced by the air-jet system, as is apparent at station 2. The difference in the distortion attenuation between the fan and core streams is also apparent at station 2.3, as is the amplification of distortion that occurred at the hub of station 3.

The centerline of the paths taken by the distorted areas of the measured flow properties are shown plotted in figure 6. Also shown are the relative locations of the inlet distorted sector, the mean streamline flow path calculated from the stage vector diagrams for the fan and compressor streams, and the direction of rotor rotation. Note that the distorted areas do not propagate along the streamline path as might be expected. Any conjecture as to the propagation mechanisms, or the influence that the design characteristics of the particular compressor have is beyond the scope of this paper. In the core stream, the property lines tracked in seemingly random directions, and were usually displaced circumferentially from each other. For instance, the line of elevated temperature was displaced approximately 90 degrees circumferentialy in the direction of rotor rotation from the total pressure defect line throughout much of the core stream. In the fan stream, however, these two lines were nearly coincident. It was also noted that a 2 per rev (2-lobe) variation in flow velocity was generated in the fan stream. In the high pressure compressor, a 2-lobe variation in pressure was generated. The lower lobe shown in figure 6(b) was located downstream of the region of the hub distortion amplification at station 3. This 2-lobe variation in pressure was difficult to track, however, because of the low amplitude of distortion in the nigh pressure compressor.

The amount of rotation also varied radially, as shown in cross-section in figure 7. This radial variation in rotation resulted in a considerable skew to the total pressure and velocity distorted sectors at stations 2.3 and 3. The skew resulted in a predominate tip radial defect in velocity which extended down to the hub between 100 and 250 degrees, where the

hub distortion amplification occurred. The location of the hub amplification coincided approximately with one of the areas of low static pressure at station 3.

The relative differences in orientation between the areas of pressure and temperature distortion are also apparent in figure 7. The effect of the orientation and amplitude of this combined distortion in pressure and temperature on compressor stability has been the subject of several Lewis programs on simple and complex compressor systems. The results obtained thus far are published in references 4 and 5.

In figure 8 is shown the comparisons between the average absolute flow velocities measured with and without inlet distortion. The results show almost no differences except at the high compressor exit, station 4, where an approximate 20 percent reduction in flow velocity was measured with inlet distortion.

There was also a relatively small change in the speed ratio between the low and high speed rotors due to the inlet distortion. There was, however, a general reduction in the core stream pressure ratio and efficiency, and in bypass ratio of between 2 and 3 percent. These differences are shown in figure 9 as ratios to the measured performance with an undistorted inlet.

Surge Characteristics

In order to locate and follow the sequence of events which occurred during surge, many high response total and static pressure transducers were located on both sides of the compressor system (180 degrees opposed) at each rating station. Analysis of these data was found to be difficult and conflicting because of the sudden and wide-spread level of dynamic activity just before and during surge. However, some of the more significant events could be identified, such as is illustrated in the example of figure 10. A stall-recovery occurring between stations 2.3 and 3 would appear as a simultaneous mirror-image pulse in pressure at these two stations, indicating a momentary breakdown or blockage in the flow somewhere between the two stations. If it were a rotating stall cell, a similar pattern would appear on the opposite side of the compressor, arriving there at a rotative speed of approximately half the rotor mechanical speed.

A surge (nonrecoverable or terminal stall) would initially

appear in the same form as a stall-recovery, however the pressures would not recover. This is illustrated in figure 10 between stations 3 and 4. At surge, complete breakdown of the flow and drop off of pressure occurs. This allows the higher pressures of the downstream stages to vent forward through the compressor in the form of a pressure wave or hammershock. The subsequent movement of the wave as it passes each station is illustrated as the last event on the figure.

The actual sequence of events which occurred during surge are shown in figure 11 for an undistorted inlet, and figure 12 for a distorted inlet. They show the rapidity and apparent randomness of the events. For the undistorted inlet, figure 11, a rapid series of surges occurred at various points within or adjacent to the low pressure compressor over a period of 3 milliseconds. Evidence of the complete breakdown of flow during this period was the emergence a few milliseconds later of a hammershock wave, starting at the front end of the high pressure compressor and proceeding forward to the inlet.

With a distorted inlet, figure 12, the initial event was a momentary stall-recovery in the tip region on the undistorted (right) side behind station 3. This stall recovery at the tip was followed in rapid succession by a momentary stall-recovery at the hub behind station 2.3 on the same side, and a surge within the high pressure compressor on the left side. This latter event had the combined effect of initiating a hammershock wave on the left side of the high pressure compressor, as well as rotating to the right side of the compressor at half rotor speed and causing that side to surge and hammershock.

The above events can only be compared to each other, or compared to the steady-state flow conditions noted in the previous section in the most general of terms. First, a rapid series of surges occured for the undistorted inlet case, or stall-recoveries and surges for the distorted inlet case. This activity was located primarily in the forward half of the compressor system for the undistorted inlet case, and the rear half for the distorted inlet case. For the distorted inlet case, the stall-recovery activity was located just downstream of the two stations where the amplification of the static pressure and total pressure distortion was the greatest, stations 2.3 and 3, respectively.

CONCLUDING REMARKS

Presented herein are the flow characteristics obtained experimentally for the compression system of a 2-spool afterburning turbofan engine operating with 180 degree distortion in inlet total pressure. Analysis of results are currently in process, however a few generalized conclusions can be drawn from the data.

1. The compression system exhibited a strong pumping effect on the distorted flow; that is, the distorted and undistorted sides of the system tended to operate at the same Mach No. The result was an amplification in the static pressure distortion to approximately the level of the total pressure distortion entering the fan and low pressure compressor.

2. The plenum effect of the relatively large volumes at the exit of the fan, low,and high pressure compressor, reduced the amplitude of the static pressure distortion to near zero. As a result, the total pressure distortion of the flow was attenuated as it approached these stations.

3. Distortion amplification occurred at the hub region of the low pressure compressor due possibly to some localized effect, such as hub cavity cross-flows, or the hub pumping characteristics.

4. The distorted inlet sector did not propagate in the axial direction or along a streamline flow path, but in seemingly random directions as it progressed through the compressor system.

5. The overall performance of the compression system with inlet distortion did not change substantialy from its clean inlet performance. The observed differences were a 2 to 3 percent reduction in pressure ratio, efficiency, and bypass ratio, and a 20 percent reduction in core stream average exit velocity.

6. With inlet distortion, the majority of the dynamic activity leading up to flow breakdown and surge occurred in the high pressure compressor. Without inlet distortion, it occurred in the low pressure compressor.

APPENDIX A - SYMBOLS

BPR	Bypass ratio, $(W_2 - Wc)/Wc$
N	Rotative speed
PT	Absolute total pressure
PS	Static pressure
RNI	Reynolds Number Index, $(\delta/(\mu/\mu_{standard})\sqrt{\theta})_2$
T	Absolute total temperature
V	Absolute flow velocity
W	Air mass flow
Δ	Maximum - minimum
δ	PT/PT, standard
η	Adiabatic total efficiency
θ	T /(T standard)
μ	Absolute viscosity

SUBSCRIPTS

C	Core stream, sta 2 to 4
F	Fan stream
H	High speed rotor
L	Low speed rotor
M	Mean radius
T	Tip radius
$\overline{(\ )}$	Ring average (Station average, figure 5)

2	Engine inlet station
2.3	Fan rotor exit station
3	High pressure compressor inlet
4	High pressure compressor exit

REFERENCES

1. Harley, K. G., Burdsall, E. A.: "High Loading Low-Speed Fan Study II. Data and Performance, Unslotted Blades and Vanes." NASA CR-72667, PWA 3653, May 1970.

2. Morris, A. L., Sulam, D. H.: "High-Loading 1800 ft/sec Tip Speed Transonic Compressor Fan Stage, II. Final Report." NASA CR-120991 PWA-4463, Dec., 1972.

3. Koch, C. C., Bilwakesh, K. R., Doyle, V. L.: "Evaluation of Range and Distortion Tolerance for High Mach Number Transonic Fan Stages, Vol. I, Task I Stage Final Report." NASA CR-72806, GE R71 AEG-133, August 1971.

4. Braithwaite, W. M., Graber, E. J., Mehalic, C. M.: "The Effects of Inlet Temperature and Pressure Distortion on Turbojet Performance." NASA TMX-71431, November 1973, AIAA 73-1316.

5. Graber, E. J., Braithwaite, W. M.: "Summary of Recent Investigations of Inlet Flow Distortion Effects on Engine Stability." NASA TMX-71505, January 1974, AIAA 74-236.

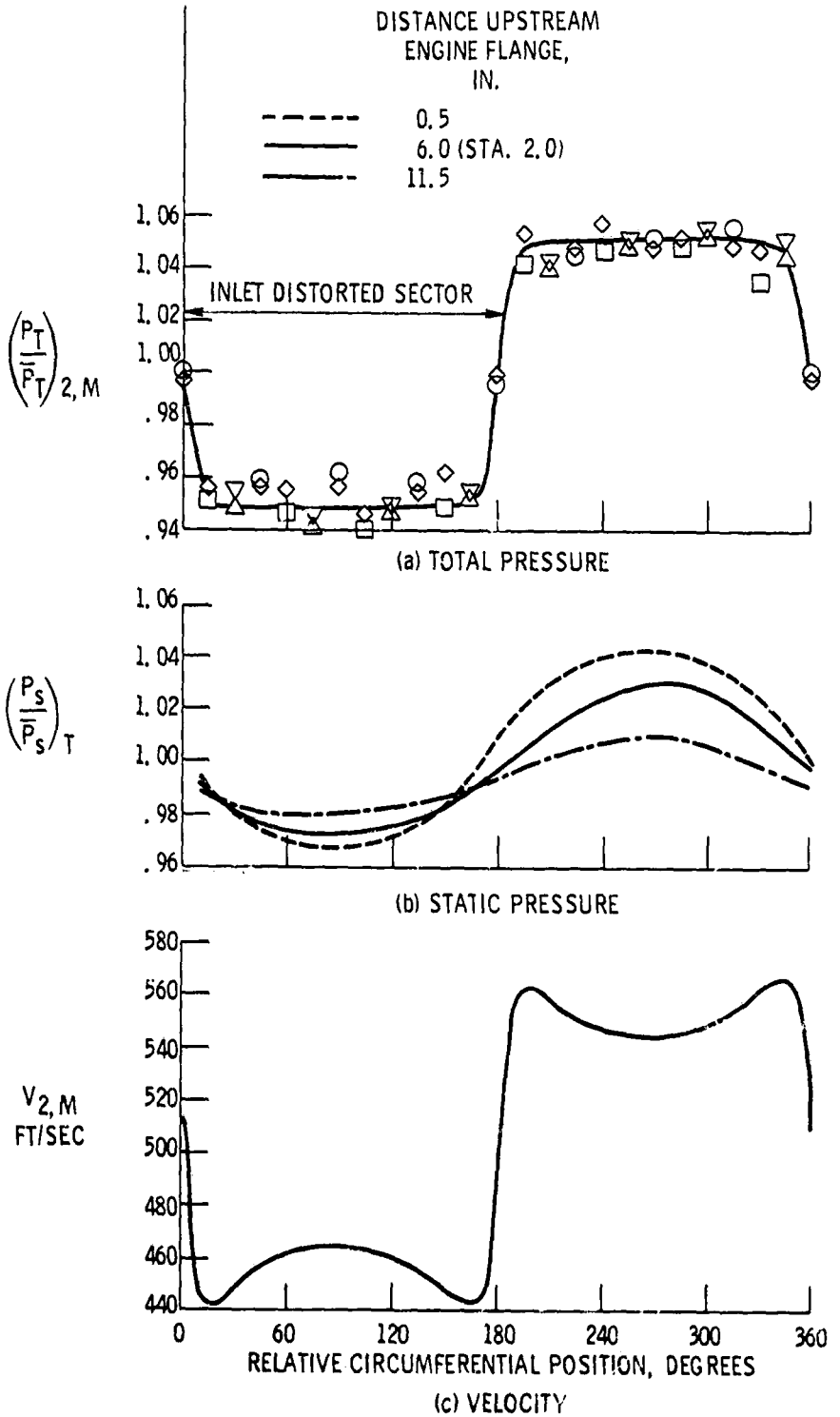

Figure 2. - Inlet flow measurements with distortion, $(\Delta P_T/\bar{P}_T)_2$ = 9 percent.

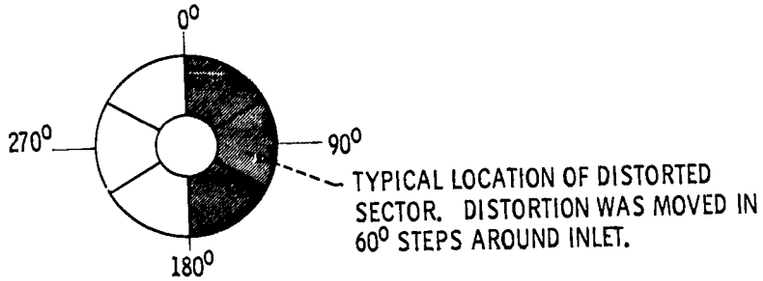

CROSS-SECTION AT STATION 2

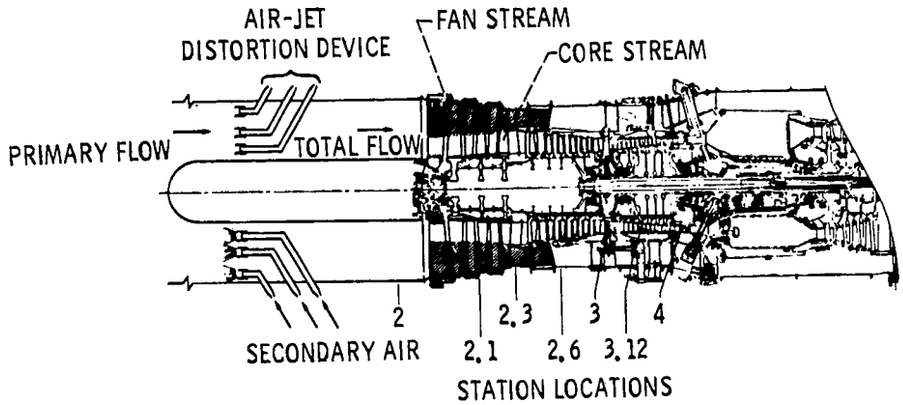

Figure 1. - Facility inlet and engine compression system.

E-3013

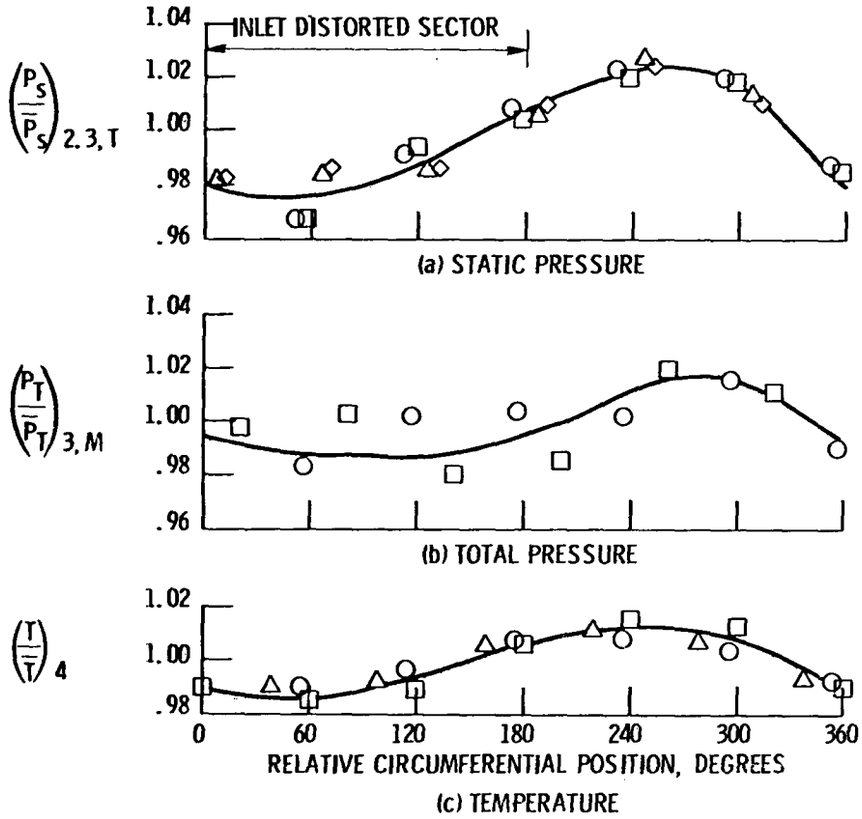

Figure 3. - Typical inner-compressor flow measurements with inlet distortion, $(\Delta P_T/\bar{P}_T)_2 = 9$ percent.

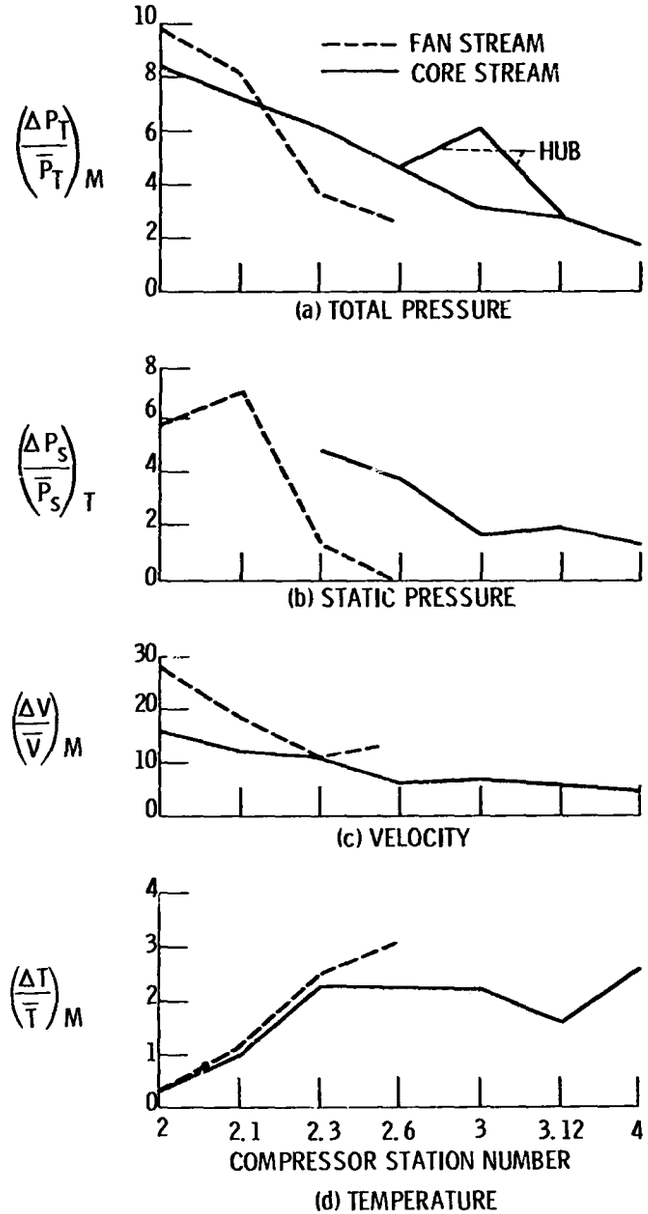

Figure 4. - Distortion attenuation, $(\Delta P_T/\bar{P}_T)_2 = 9$ percent.

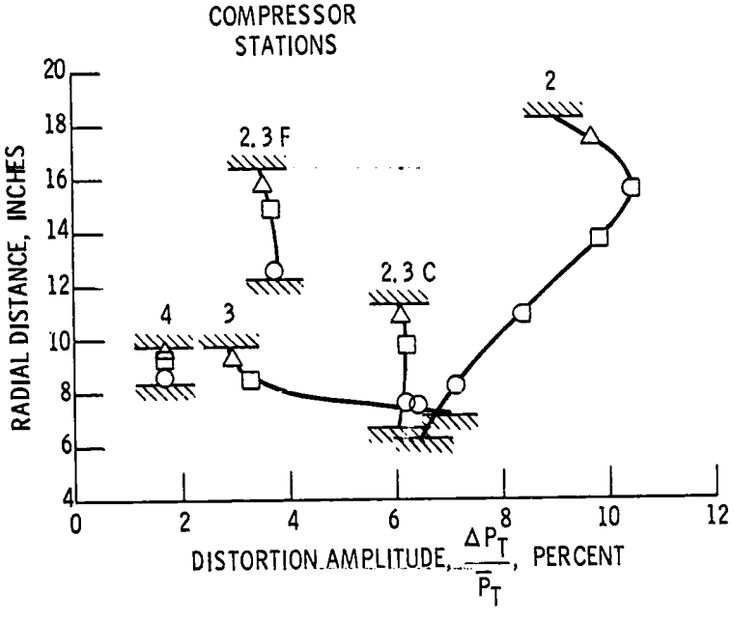

Figure 5. - Radial variation in distortion amplitude, $(\Delta P_T/\bar{P}_T)_2$ = 9 percent.

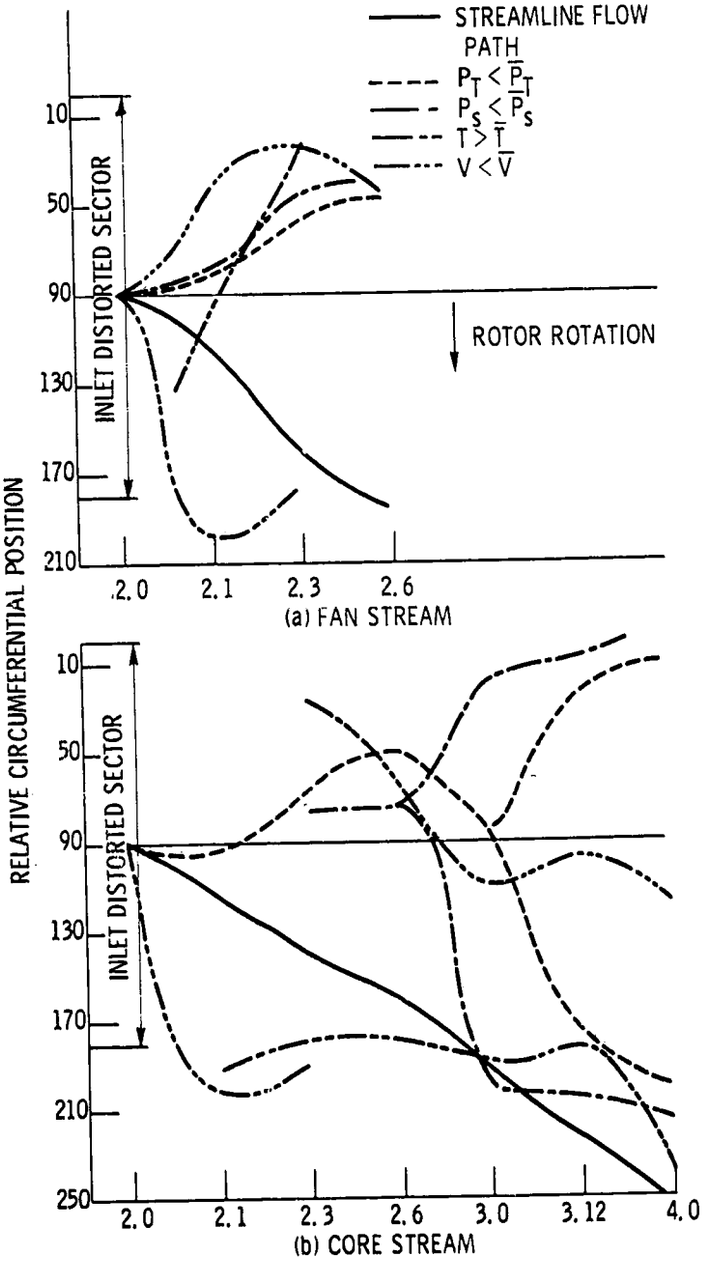

Figure 6. - Rotation of center of defect areas, $(\Delta P_T/\bar{P}_T)_2$ = 9 percent.

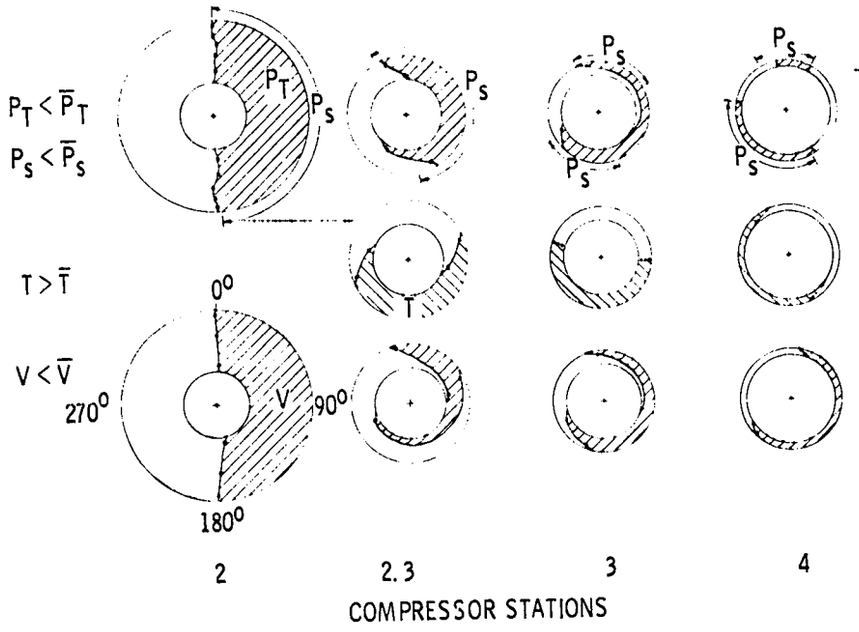

Figure 7. - Spacial variation of distorted sectors, looking upstream (clockwise rotor rotation).

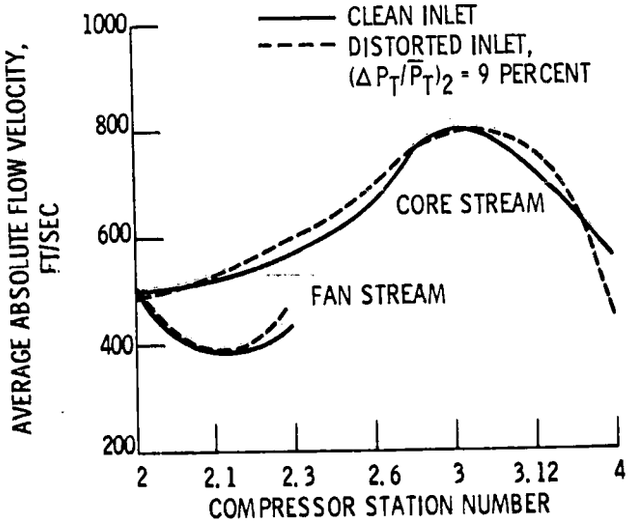

Figure 8. - Axial variation in absolute flow velocity.

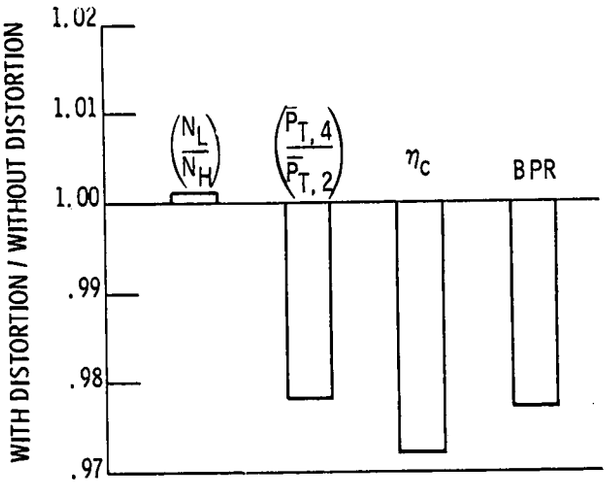

Figure 9. - Distortion effects on overall compressor performance, $(\Delta P_T/\bar{P}_T)_2 = 9$ percent.

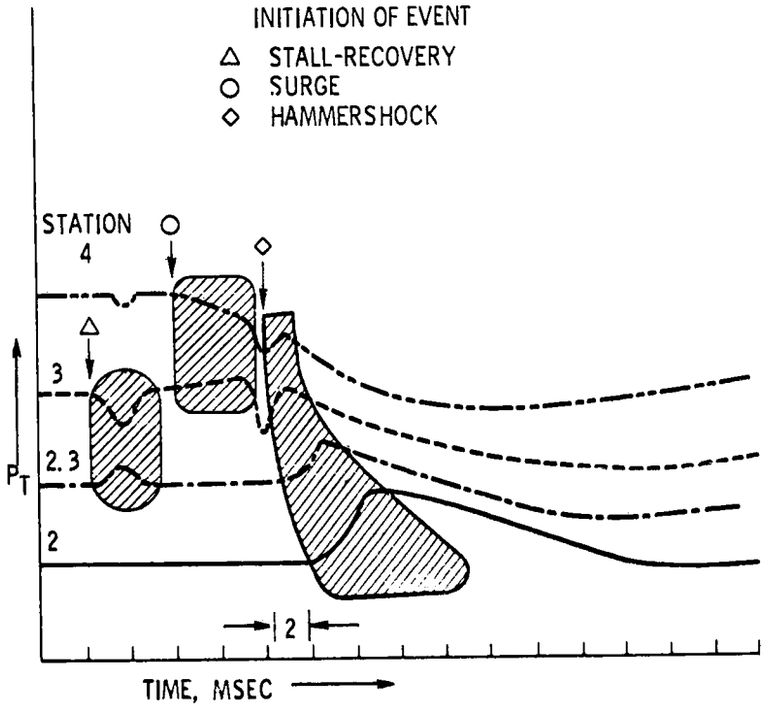

Figure 10. - Typical high response pressure traces.

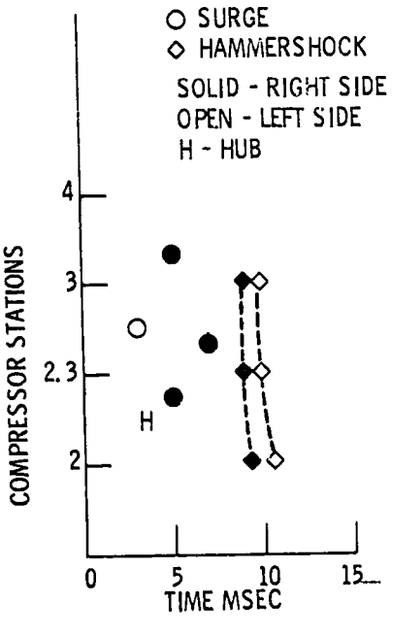

Figure 11. - Dynamic activity with undistorted inlet flow.

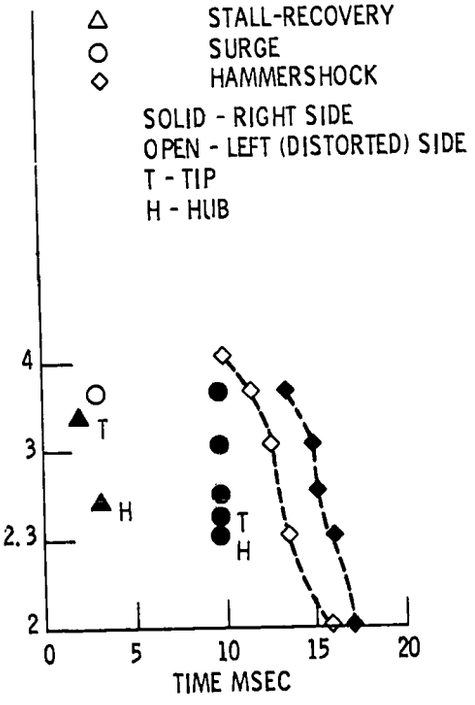

Figure 12. - Dynamic activity with distorted inlet flow, $(\Delta P_T/\overline{P}_T)_2$ = 13 percent.

NASA-Lewis